Séminaire Laurent Schwartz

EDP et applications

Année 2013-2014

Kazuo Aoki and Tetsuro Tsuji

Moving boundary problems in kinetic theory of gases: Spatially one-dimensional problems

Moving boundary problems in kinetic theory of gases: Spatially one-dimensional problems

Kazuo Aoki[1] and Tetsuro Tsuji[2]

[1]Department of Mechanical Engineering and Science, Kyoto University
[2]Department of Mechanical Science and Bioengineering, Osaka University

Abstract Unsteady flows of a rarefied gas in a full space caused by an oscillatory motion of an infinitely wide plate in its normal direction is investigated numerically on the basis of the Bhatnagar-Gross-Krook (BGK) model of the Boltzmann equation. The present notes aim at showing the properties and difficulties inherent to moving boundary problems in kinetic theory of gases using a simple one-dimensional setting.

1 Introduction

Gases in low-pressure circumstances and in microscales, in which the mean free path of the molecules is not negligibly small compared with the characteristic length of the system, are in general not in local thermal equilibrium. Therefore, their behavior cannot be described by ordinary macroscopic fluid dynamics that assumes the local thermodynamic equilibrium. For such gases, molecular gas dynamics, the gas dynamics based on kinetic theory, has to be used. The basic equation of molecular gas dynamics is the celebrated Boltzmann equation for the molecular velocity distribution function, which is a complicated nonlinear integro-differential equation (e.g., [1, 2, 3]).

Numerical analysis of moving-boundary problems for the Boltzmann equation is one of the hot topics in molecular gas dynamics in connection with MEMS (micro electro mechanical systems) applications. The most prevailing numerical solution method for the Boltzmann equation is the DSMC (direct simulation Monte Carlo) method [4], which is a particle and stochastic method. However, as is well known, this method has a difficulty in solving time-dependent problems because of the statistical noise inherent to it. Since moving-boundary problems are essentially time dependent, this method is not suitable for moving-boundary problems. For this reason, deterministic solution methods, such as finite-difference and finite-volume methods, combined with CFD (computational fluid dynamics) techniques, such as moving-lattice techniques and the immersed boundary method, have been attempted. However, some care should be exercised because of the difference in structure between the Boltzmann and fluid-dynamic equations.

In time-independent boundary-value problems, when the boundary is convex toward the domain of the gas, the velocity distribution function is discontinuous on the boundary, and the discontinuity propagates into the gas along the characteristic line of the Boltzmann equation [5, 2, 3]. In the case of a planar boundary, the discontinuity does not propagate into the gas as long as no external force is acting

on the gas molecules. However, if the planar boundary is moving with acceleration/deceleration in its normal direction (for example, an oscillatory motion), the discontinuity on the boundary in general propagates into the gas. To the best of the authors' knowledge, there is no study focusing attention on this point.

In the present notes, we restrict ourselves to the spatially one-dimensional case in which a plane boundary makes an oscillatory motion in its normal direction. We describe the singularities in the velocity distribution function caused by the motion of the boundary and give an outline of the numerical method that captures the singularity. The notes are based on the authors' recent works [6, 7].

2 Boltzmann equation and discontinuity in velocity distribution function

2.1 Spatially one-dimensional problems

The velocity distribution function of gas molecules, which is in general a function of the space variable x_i, the molecular velocity ζ_i, and the time variable t, expresses the mass density of the gas molecules in the six-dimensional phase space (x_i, ζ_i) at time t. It is denoted by $f(x_i, \zeta_i, t)$. All the macroscopic quantities are expressed as its moments. For example, the density $\rho(x_i, t)$, the flow velocity $v_i(x_i, t)$, temperature $T(x_i, t)$, and pressure $p(x_i, t)$ of the gas are given as follows:

$$\rho = \int_{\mathbb{R}^3} f d\boldsymbol{\zeta}, \tag{1a}$$

$$v_i = \frac{1}{\rho} \int_{\mathbb{R}^3} \zeta_i f d\boldsymbol{\zeta}, \tag{1b}$$

$$T = \frac{p}{R\rho} = \frac{1}{3R\rho} \int_{\mathbb{R}^3} (\zeta_i - v_i)^2 f d\boldsymbol{\zeta}, \tag{1c}$$

where R is the gas constant per unit mass and $d\boldsymbol{\zeta} = d\zeta_1 d\zeta_2 d\zeta_3$.

Let us consider spatially one-dimensional problems, such as the case in which an infinitely wide plate makes an arbitrary motion in its normal direction. Then, if we take the x_1 axis perpendicular to the plate, f depends neither on x_2 nor on x_3, i.e., $f(x_1, \zeta_i, t)$, and the Boltzmann equation can be written in the following form:

$$\frac{\partial f}{\partial t} + \zeta_1 \frac{\partial f}{\partial x_1} = J(f, f), \tag{2}$$

where $J(f, f)$ is the Boltzmann collision operator, which is quadratically nonlinear in f and contains five-fold integral. Its explicit form is omitted here (see, e.g., [1, 2, 3]).

As the initial condition for Eq. (2), we specify the velocity distribution function at $t = 0$, i.e.,

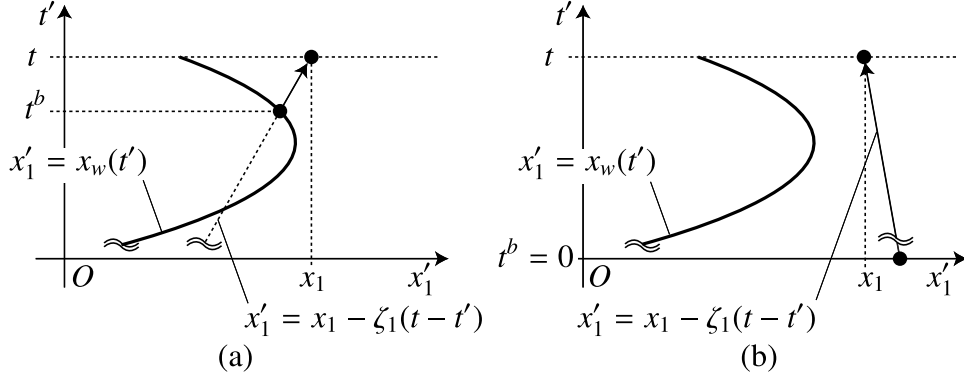$$f(x_1, \zeta_i, 0) = f_{\text{in}}(x_1, \zeta_i). \tag{3}$$

Fig. 1: The (x'_1, t') plane and the trajectory of the plate [7]. (a) The case where the characteristic line meets the trajectory, (b) the case where the characteristic line does not meet the trajectory.

On the other hand, as the boundary condition for Eq. (2), we specify the velocity distribution function for the gas molecules reflected on the plate according to the model of the interaction between the gas molecules and the boundary. Here, we assume the conventional diffuse reflection condition. That is, the velocity of the reflected molecules is distributed according to the (half-range) Maxwellian distribution based on the temperature and velocity of the boundary, and there is no net mass flux across the boundary (cf. [1, 2, 3]). Let the infinitely wide plate be located at $x_1 = x_w(t)$, and let the velocity of the plate be $v_w(t) = dx_w(t)/dt$. When the gas is on the right side of the plate [i.e., the side for $x_1 > x_w(t)$], the diffuse reflection condition can be written as

$$f = \frac{\sigma_w}{(2\pi R T_w)^{3/2}} \exp\left(-\frac{[\zeta_1 - v_w(t)]^2 + \zeta_2^2 + \zeta_3^2}{2R T_w}\right)$$
$$[\,\zeta_1 - v_w(t) > 0, \quad x_1 = x_w(t)\,], \tag{4a}$$

$$\sigma_w = -\sqrt{\frac{2\pi}{R T_w}} \int_{\zeta_1 - v_w(t) < 0} [\zeta_1 - v_w(t)] f \, d\boldsymbol{\zeta}, \tag{4b}$$

where T_w is the temperature of the plate. When the gas is on the left side [i.e., the side for $x_1 < x_w(t)$], $\zeta_1 - v_w(t)$ should be replaced with $v_w(t) - \zeta_1$ in Eqs. (4a) and (4b).

2.2 Formation of discontinuities

In this subsection, we consider the (x_1, t) plane. But, for convenience for explanation, we call this plane the (x'_1, t') plane using the current coordinates x'_1 and t' and express a point fixed in the plane by (x_1, t) (Fig. 1). Therefore, the trajectory of the plate is expressed as $x'_1 = x_w(t')$ (Fig. 1). The derivative terms of the Boltzmann equation (2) are contained only on the left-hand side, so that its solution f is determined along the characteristic line of the left-hand side, that is, along the trajectory
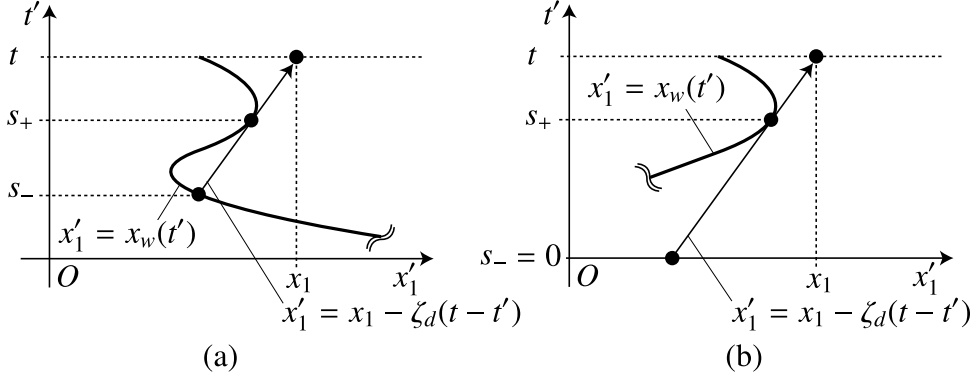
Fig. 2: The characteristic line tangent to the trajectory of the plate and the discontinuity [7]. (a) The case where the characteristic line meets the trajectory, (b) the case where the characteristic line does not meet the trajectory.

of gas molecules. The characteristic line passing the point (x_1, t) in the (x'_1, t') plane is given by $x'_1 = x_1 - \zeta_1(t - t')$. If we trace back in time the characteristic line form the point (x_1, t), either we meet the trajectory of the plate at time $t' = t^b$ [Fig. 1(a)] or we reach the initial time $t' = 0$ without meeting it [Fig. 1(b); we set $t^b = 0$ in this case], depending on the value of ζ_1. Since the unknown function f is contained both in the right-hand side of Eq. (2) and in σ_wmEq. (4b)] in the boundary condition (4a), it is not so simple. But, in the case of Fig. 1(a), the value of f at the point (x_1, t) is conceptually determined along the characteristic line in the direction of the arrow staring from the boundary condition (4a) at the time $t' = t^b$ in the past. In the case of Fig. 1(b), the starting point is the initial condition. In the operation of tracing back in time, the other components ζ_2 and ζ_3 only play the role of parameters. Therefore, in the following, we discuss on the basis of (x_1, ζ_1, t) supposing that ζ_2 and ζ_3 are fixed appropriately.

Let us suppose that the characteristic line at a molecular velocity component $\zeta_1 = \zeta_d$ is tangent to the trajectory of the plate (Fig. 2). In the situation shown in Fig. 2(a), the characteristic line corresponding to ζ_1 slightly larger than ζ_d originates from the plate at the time slightly after (or, in the figure, slightly above) s_+, whereas the characteristic line corresponding to ζ_1 slightly smaller than ζ_d originates from the plate at the time slightly before (or, in the figure, slightly below) s_-. The values of f at the point (x_1, t) determined along these two characteristic lines are in general different because the situation at the starting point as well as the length of the characteristic line reaching the point (x_1, t) is different. In other words, if f at (x_1, t) is regarded as a function of ζ_1, then it is discontinuous at $\zeta_1 = \zeta_d$. This discontinuity, which decays because of the collisions between the gas molecules, is not visible when the time interval $t - s_+$ is sufficiently larger than the mean free time of the gas molecules. It would be obvious that the discontinuity is formed also in the situation shown in Fig. 2(b). This mechanism forming the discontinuity is similar to that known for a steady gas around a convex boundary (convex toward the gas domain) [5, 2, 3].

2.3 Numerical method

As can be understood from the explanation given above, in problems in which the plate starts oscillation at the initial time, the velocity distribution function at a point just outside the maximum amplitude of the plate exhibits a complex shape as time proceeds because of the localized discontinuities. In order to capture the complex shape accurately, we have to obtain all the characteristic lines that are tangent to the trajectory of the plate in the past and integrate the equation numerically along both sides of each of such characteristic lines. In addition, it is known that the variation of f is steep for the molecular velocities in the vicinity of the discontinuities, so that we have to use a grid system for ζ_1 that concentrates in the neighborhood of the discontinuities. The reader is referred to [7] for the details of the numerical method, including the treatment of singularities weaker than the discontinuities.

The complexity of the collision operator of the Boltzmann equation makes accurate numerical solution for delicate problems by deterministic methods extremely hard. For this reason, model Boltzmann equations with simplified collision operators are often used. In the following, we will show some results based on one of such models, the so-called BGK model [8, 9], in which the collision operator $J(f, f)$ in Eq. (2) is replaced by the following $J_{\mathrm{BGK}}(f)$:

$$J_{\mathrm{BGK}}(f) = A_c \rho \left(f_e - f \right) \tag{5}$$

where

$$f_e = \frac{\rho}{(2\pi RT)^{3/2}} \exp\left(-\frac{(\zeta_i - v_i)^2}{2RT} \right), \tag{6}$$

and ρ, v_i, and T are the moments of the unknown f given by Eq. (1). However, the discussions in 2.2 are valid irrespective of the models of the collision operator (as long as an appropriate cut-off is assumed for the intermolecular potential for the Boltzmann collision operator).

3 Some results of numerical analysis

In this section, we consider two problems, the propagation of disturbances in the gas induced by a plate with a forced oscillation (propagation of nonlinear acoustic waves) and the decay of a motion of freely oscillating plate caused by the drag force exerted by the surrounding gas, and show some examples of the numerical results.

3.1 Problems

[Problem 1] (forced oscillation): The plate starts a harmonic oscillation at $t = 0$ according to $x_w(t) = a\cos\omega t$. Here, a is the amplitude, and ω is the angular frequency. We investigate the unsteady motion in the semi-infinite expanse of the gas $[x_1 > x_w(t)]$ in contact to the plate.

[Problem 2] (free oscillation): An infinitely wide plate without thickness is placed in an infinite expanse of the gas ($-\infty < x_1 < \infty$). The plate is subject to a restoring force in the x_1 direction obeying Hooke's law, i.e., $F_h = -\omega^2 \mathcal{M} x_w(t)$ per unit area, where $\mathcal{M}$ is the mass of the plate per unit area, ω is a constant, and $x_1 = 0$ indicates the equilibrium position of the plate. If the plate is displaced until $x_1 = a$ and released at time $t = 0$ without the initial velocity, the plate in general starts an oscillatory motion, which decays as time proceeds because of the drag exerted by the surrounding gas. We investigate the decay process.

In both problems, we assume that the temperature of the plate is T_0, and the gas is initially in the equilibrium state at rest at temperature T_0 and density ρ_0. Problem 2 is a coupling problem in which the motion of the gas and that of the plate interact each other.

3.2 Numerical results for forced oscillation

We first show some results for Problem 1. For convenience in the following, we define the marginal velocity distribution function $g(x_1,\, \zeta_1,\, t)$ by

$$g(x_1,\, \zeta_1,\, t) = \int_{-\infty}^{\infty} \int_{-\infty}^{\infty} f(x_1,\, \zeta_i,\, t)\, d\zeta_2 d\zeta_3. \tag{7}$$

In addition, we introduce suitable dimensionless variables based on the reference time $1/\omega$ and the reference length c_0/ω, where $c_0 = \sqrt{2RT_0}$. More specifically, we denote the dimensionless quantities corresponding to $(t,\, x_i,\, \zeta_i,\, x_w,\, \rho,\, u_1,\, T,\, p,\, a,\, g)$ by putting a bar above and define them as follows:

$$
\begin{aligned}
&\bar{t} = t/(1/\omega), \quad \bar{x}_i = x_i/(c_0/\omega), \quad \bar{\zeta}_i = \zeta_i/c_0, \\
&\bar{x}_w = x_w/(c_0/\omega), \quad \bar{\rho} = \rho/\rho_0, \quad \bar{u}_1 = u_1/c_0, \\
&\bar{T} = T/T_0, \quad \bar{p} = p/R\rho_0 T_0, \\
&\bar{a} = a/(c_0/\omega), \quad \bar{g} = g/\rho_0 c_0.
\end{aligned}
\tag{8}
$$

Further, l_0 denotes the mean free path of the gas molecules in the equilibrium state at rest at temperature T_0 and density ρ_0 [for the BGK model, $l_0 = (2/\sqrt{\pi})(c_0/A_c \rho_0)$, where A_c is the constant such that $A_c \rho_0$ indicates the collision frequency of the gas molecules at the same equilibrium state], and $\mathrm{Kn} = l_0/(c_0/\omega)$ the Knudsen number. In what follows, we use the following K as the measure of gas rarefaction in place of Kn:

$$\mathsf{K} = (\sqrt{\pi}/2)\mathrm{Kn}, \tag{9}$$

We note that Eqs. (7)–(9) are common to Problem 2.

3.2.1 Velocity distribution function

In Fig. 3, we show the marginal velocity distribution function $\bar{g}(\bar{x}_1,\, \bar{\zeta}_1,\, \bar{t})$ as a function of $\bar{\zeta}_1$ for $\mathsf{K} = 10$ and $\bar{a} = 1$. The upper figures are at $\bar{t} = 15\pi$ and the lower
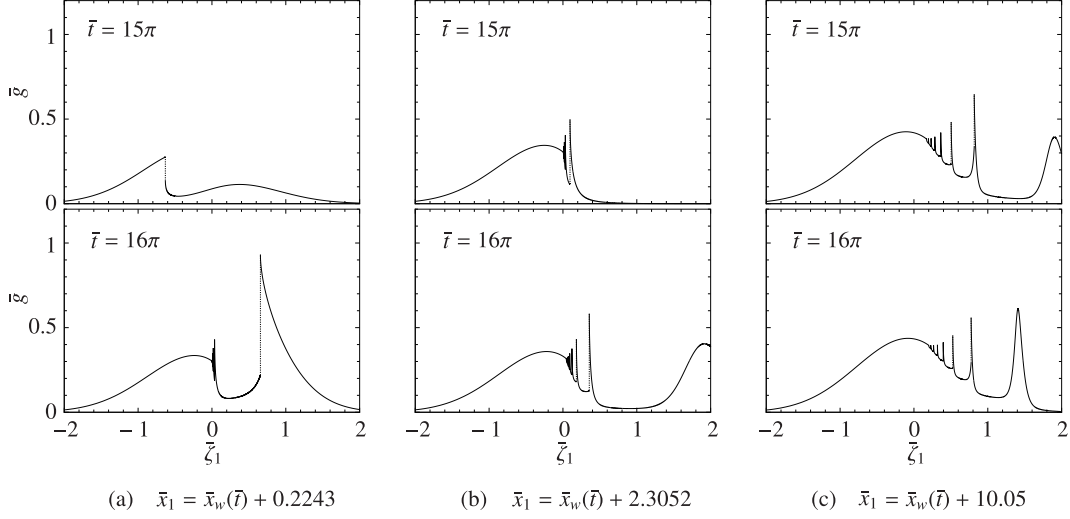
(a) $\bar{x}_1 = \bar{x}_w(\bar{t}) + 0.2243$ (b) $\bar{x}_1 = \bar{x}_w(\bar{t}) + 2.3052$ (c) $\bar{x}_1 = \bar{x}_w(\bar{t}) + 10.05$

Fig. 3: $\bar{g}(\bar{x}_1, \bar{\zeta}_1, \bar{t})$ ($\mathsf{K} = 10 \mathrm{C}\bar{a} = 1$) [7]D (a) $\bar{x}_1 = \bar{x}_w + 0.2243$, (b) $\bar{x}_1 = \bar{x}_w + 2.3052$, (c) $\bar{x}_1 = \bar{x}_w + 10.05$. The upper figures are at $\bar{t} = 15\pi$, and the lower figures at $\bar{t} = 16\pi$.

figures at $\bar{t} = 16\pi$, and panel (a) shows the result near the plate: $\bar{x}_1 = \bar{x}_w + 0.2243$, panel (b) that slightly apart from the plate: $\bar{x}_1 = \bar{x}_w + 2.3052$, and panel (c) that further away from the plate: $\bar{x}_1 = \bar{x}_w + 10.05$. Since the gas is relatively rarefied ($\mathsf{K} = 10$), the effect of collisions between gas molecules is small, so that the discontinuities explained in Sec. 2.2 do not decay rapidly. Therefore, many discontinuities as well as the sharp peaks around them can be observed clearly. The shape of the velocity distribution function near the plate [Fig. 3(a)] changes significantly during a half period ($\bar{t} = 15\pi \to 16\pi$), and in the lower figure, it is seen that the discontinuities accumulate and are localized in the vicinity of $\bar{\zeta}_1 = 0$. As the distance from the plate increases [Fig. 3(b) $\to$ Fig. 3(c)], the peaks separate, and the discontinuities closer to $\bar{\zeta}_1 = 0$ decay more rapidly.

For a free-molecular gas in which there are no collisions between the gas molecules ($\mathsf{K} = \infty$), infinitely many peaks accumulate without decay. In contrast, for $\mathsf{K} = 1$, where the effect of collisions is larger, the decay of the discontinuities is fast. In fact, almost no peak is seen in the far field corresponding to Fig. 3(c), and only a few discontinuities are observed even near the plate corresponding to Fig. 3(a). These results are omitted in this article. The reader is referred to [7].

The complex and steep shape as shown in Fig. 3 is not expected to be captured accurately by the conventional solution methods, such as the finite-difference and finite-volume methods.

3.2.2   Macroscopic quantities

In Problem 1, the oscillation of the plate propagates into the gas in the form of a wave. When the gas is rarefied, as in the case of Fig. 3, the oscillation in the macroscopic quantities attenuates quickly as the distance from the plate increases

(see [6]). Therefore, we show the results for less rarefied cases. Figure 4 shows the profiles of the macroscopic quantities $\bar{\rho}$, $\bar{u}_1$, $\bar{T}$, and $\bar{p}$ during the 20th period ($\bar{t}/2\pi = 19 \to 20$) [panel (a)] or 80th period ($\bar{t}/2\pi = 79 \to 80$) [panel (b)], panel (a) being for the slightly rarefied regime (K = 0.05) and panel (b) for the transition regime (K = 2). In Fig. 4(a), the formation of waves of saw-tooth shape, whereas Fig. 4(b) it is not seen because the waves attenuate quickly with the distance from the plate.
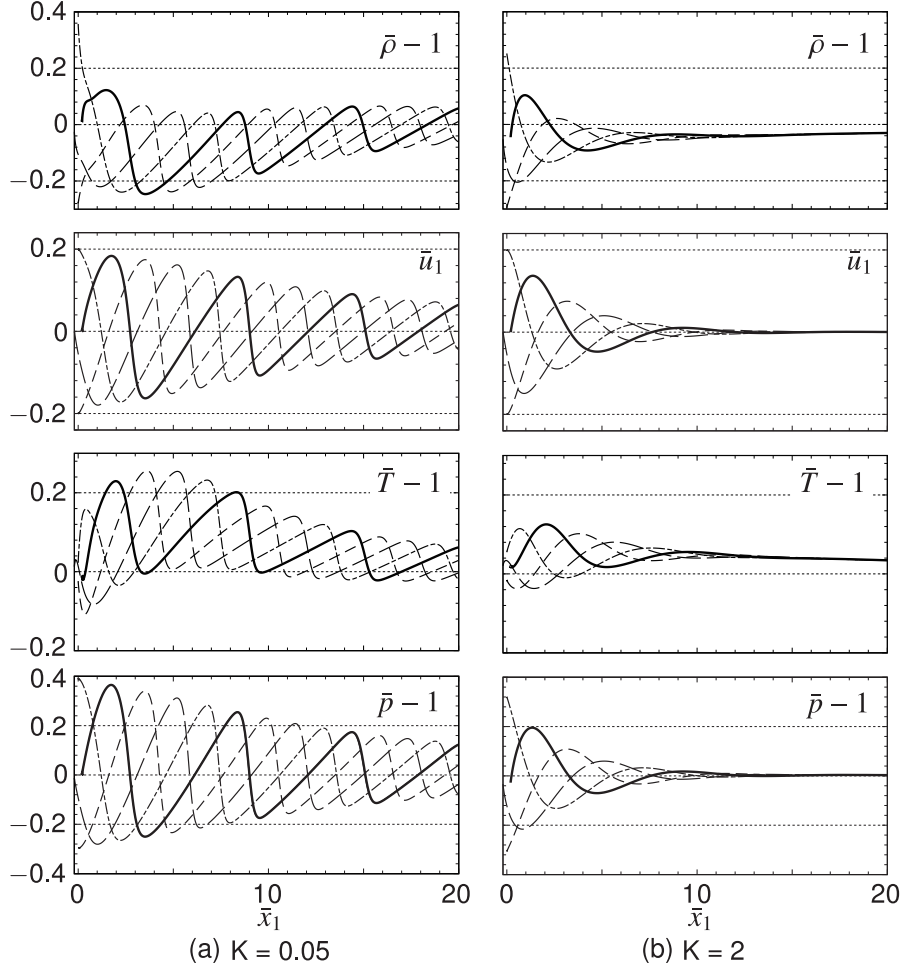

(a) K = 0.05 (b) K = 2

Fig. 4: Profiles of $\bar{\rho}$, $\bar{u}_1$, $\bar{T}$, and $\bar{p}$ ($\bar{a} = 0.2$) [6]D (a) K = 0.05, (b) K = 2. In (a), the profiles at $\bar{t}/2\pi = 19.25$ (dashed line), 19.5 (long dashed line), 19.75, (dot-dashed line), and 20 (solid line) are shown, and in (b), those at $\bar{t}/2\pi = 79.25$ (dashed line), 79.5 (long dashed line), 79.75 (dot-dashed line), 80 (solid line) are shown.

Now, let $h(\bar{x}_1, \bar{t})$ be an arbitrary (dimensionless) macroscopic quantity ($h = \bar{\rho}$, $\bar{u}_1$, $\bar{T}$, etc.) and let $h_{av}(\bar{x}_1, \bar{t})$ denote its average over a period of oscillation of the plate from $\bar{t} - 2\pi$ to $\bar{t}$, i.e.,

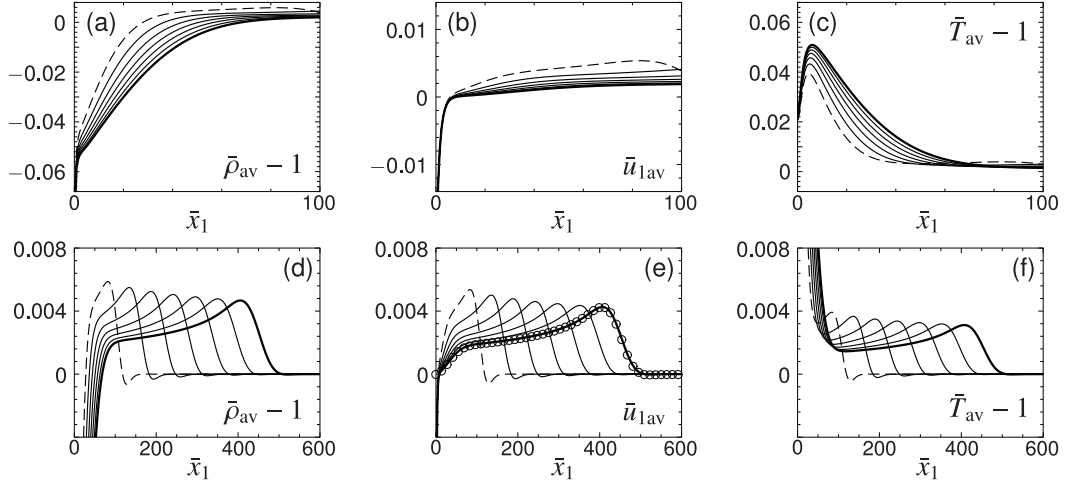$$h_{av}(\bar{x}_1, \bar{t}) = \frac{1}{2\pi} \int_{\bar{t}-2\pi}^{\bar{t}} h(\bar{x}_1, s)\, ds. \tag{10}$$

Fig. 5: Time evolution of the one-period averages, $\bar{\rho}_{\mathrm{av}}$, $\bar{u}_{1\mathrm{av}}$, and $\bar{T}_{\mathrm{av}}$ ($\mathsf{K} = 2$, $\bar{a} = 0.2$) [6]D (a), (d) $\bar{\rho}_{\mathrm{av}}$C(b), (e) $\bar{u}_{1\mathrm{av}}$, (c), (f) $\bar{T}_{\mathrm{av}}$. The profiles at $\bar{t}/2\pi = 20$ (dashed line), 30, 40, ..., 70 (solid line for all these $\bar{t}/2\pi$), and 80 (bold solid line) are shown. The upper figures [(a), (b), and (c)] show the range $0 \le \bar{x}_1 \le 100$, and the lower figures [(d), (e), and (f)] the range $0 \le \bar{x}_1 \le 600$. The circles ○ indicate the profile of $(\bar{\rho}\bar{u}_1)_{\mathrm{av}}$ at $\bar{t}/2\pi = 80$.

In Fig. 5, we show the time evolution of the one-period average of the density, flow velocity, and temperature, i.e., $\bar{\rho}_{\mathrm{av}}$, $\bar{u}_{1\mathrm{av}}$, and $\bar{T}_{\mathrm{av}}$, for $\mathsf{K} = 2$ and $\bar{a} = 0.2$. Panels (a) and (d) are for $\bar{\rho}_{\mathrm{av}}$, panels (b) and (e) for $\bar{u}_{1\mathrm{av}}$, and panels (c) and (f) for $\bar{T}_{\mathrm{av}}$; the profiles at $\bar{t}/2\pi = 20$ (dashed line), 30, 40, ..., 70 (solid line for all these $\bar{t}/2\pi$), and 80 (bold solid line) are shown; the upper figures [panels (a), (b), and (c)] show the region relatively close to the plate, whereas the lower figures [panels (d), (e), and (f)] the whole range including the wave front of the disturbance with the vertical axis magnified. The circles ○ in Fig. 5(e) indicate the profile of the one-period average of $\bar{\rho}\bar{u}_1$, i.e., $(\bar{\rho}\bar{u}_1)_{\mathrm{av}}$, at $\bar{t}/2\pi = 80$. A weak compression wave, which decays very slowly, proceeds as the wave front, and a high temperature (low density) region is formed slowly near the plate. Since the one-period average of the mass flow just behind the wave front is positive, there appears a gas flow toward infinity (acoustic stream). The behavior shown in Fig. 5 resembles the motion of the gas in a half space bounded by a stationary wall caused by a sudden increase of the wall temperature [10].

The wave propagation and the formation of the steady oscillation in a gas in a finite domain between an oscillating and a resting wall are investigated in [11].

3.3   Numerical results for free oscillation

Next, we present some results for Problem 2. We first show some preliminary results using the present method of characteristics (Sec. 3.3.1) and then give a brief remark on the more detailed results obtained more recently (Sec. 3.3.2). Our main interest
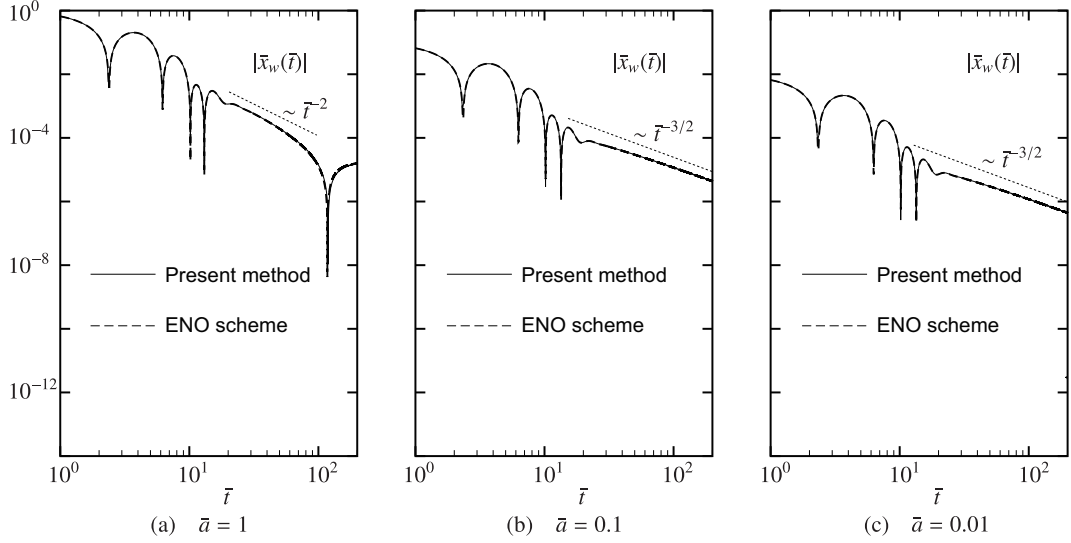
Fig. 6: Decay of the displacement $\bar{x}_w(\bar{t})$ of the plate ($\mathsf{K} = 1$) [7]D (a) $\bar{a} = 1$, (b) $\bar{a} = 0.1$, (c) $\bar{a} = 0.01$. The solid line indicates the result by the present method of characteristics, and the dashed line that by the a finite-difference method with ENO scheme.

is to know how fast the displacement $x_w(t)$ of the plate decays.

3.3.1 Results by the method of characteristics

If we assume that the drag force exerted on the plate by the surrounding gas is proportional to the velocity of the plate $v_w(t)$, then the displacement decays exponentially in time. However, if the surrounding gas is a free-molecular gas (or Knudsen gas) in which the collisions between the gas molecules are negligible, it is shown numerically that the decay is slow and is described as $|\bar{x}_w(\bar{t})| \approx \text{const} \times \bar{t}^{-2}$ [12, 13]. More precisely, the decay rate depends on the dimension d of the plate [in [13], $d = 1$ indicates the present one-dimensional problem with an infinitely wide plate, $d = 2$ the two-dimensional problem with an infinitely long plate with a finite width, and $d = 3$ the three-dimensional (axisymmetric) problem with a circular disk] and is given as $|\bar{x}_w(\bar{t})| \approx \text{const} \times \bar{t}^{-d-1}$. Incidentally, under the specular reflection boundary condition on the plate, the decay rate is rigorously proved to be $|\bar{x}_w(\bar{t})| \approx \text{const} \times \bar{t}^{-d-2}$ in the case of a monotonic decay without oscillation [14]. This slow decay in the free-molecular gas is attributed to the long-memory effect caused by the molecules that are reflected by the plate at early times and hit the plate again, with keeping their velocity, at later times (direct recollisions of the gas molecules) [14]. In fact, if we devise an artificial gas (a special Lorentz gas) in which the possibility of the direct recollisions is negligibly small, the decay is almost exponential in time and is much faster than the inverse power of time [13].

Our next question is: In the case where there are collisions between the gas molecules, i.e., in the case of a usual rarefied gas, since the possibility of the direct

recollisions with the plate is also small, does the displacement of the plate decay fast? To answer this question, we started the study of Problem 2. Figure 6 shows a preliminary result (in the sense that the computation is not made until long times) for $\mathcal{M} = 2(\rho_0 c_0/\omega)$ and $\mathsf{K} = 1$: Panel (a) is for a relatively large initial displacement $\bar{a} = 1$, and Panels (b) and (c) for smaller initial displacements. In Panel (a), the oscillation has not ceased yet, whereas in panels (b) and (c) it is likely to have ceased. The panels (b) and (c) suggest that the decay of the displacement of the plate may follow

$$|\bar{x}_w(\bar{t})| \approx \text{const} \times \bar{t}^{-3/2}, \tag{11}$$

which is, unexpectedly, even slower than in the case of the free-molecular gas.

In Fig. 6, the results using a finite-different method with the essentially non oscillatory (ENO) scheme are also shown. In the level of the velocity distribution function, the ENO scheme cannot capture discontinuities and steep changes as accurately as the present method of characteristics, in particular, for large Knudsen numbers. However, as seen from Fig. 6, the decay rate based on the ENO scheme agrees very well with that obtained by the present method. Since the present method of characteristics is computationally expensive, it is not suitable to pursue a very long-time behavior, which is necessary to clarify the decay rate of the plate. The good agreement with the ENO scheme gives some hope to obtain an accurate long-time behavior by methods other than the method of characteristics. A remark on this point will be given in the following subsection.

3.3.2   Remarks on more recent results

More recently, motivated by the good performance of the ENO scheme as shown in Fig. 6, we searched other methods which are appropriate for an accurate long-time computation. As the result, we adopted the semi-Lagrangian method proposed in [15] and carried out computation until long limes [16]. Figure 7 shows an example of the results. The mass density of the plate $\mathcal{M}$ is fixed as $\mathcal{M} = \rho_0 c_0/\omega$ in the figure. The upper figures show $\log_{10} \bar{x}_w$ versus $\log_{10} \bar{t}$ for $\bar{a} = 0.2$ [(a)], 0.01 [(b)], and 0.001 [(c)], and the lower figures the gradient $\alpha(\bar{x}_w)$ of $\log_{10}|\bar{x}_w(\bar{t})|$ with respect to $\log_{10}\bar{t}$ corresponding to the upper figures, i.e.,

$$\alpha(\bar{x}_w) = \frac{d\log_{10}|\bar{x}_w|}{d\log_{10}\bar{t}}. \tag{12}$$

The results of computation until much longer time in Fig. 7 support the decay rate (11) more convincingly. However, the curve for $\mathsf{K} = 0.4$ in Fig. 7(d) tends to deviate from the value -1.5. The curves for $\mathsf{K} = 0.4$ in Figs. 7(d)–7(f) exhibit strong oscillation after $\log_{10}\bar{t} \gtrsim 3.2$. As one can see from Figs. 7(d)–7(f), at a given large time, the displacement $|\bar{x}_w(\bar{t})|$ is smaller for smaller Knudsen number K, and for $\mathsf{K} = 0.4$, it had become less than $O(10^{-7})$ at $\log_{10}\bar{t} = 3.2$. The oscillation may be attributed to the fact that the computation had reached the limit of accuracy resolving such a small amplitude. We could say that, within the accuracy of the computation using the semi-Lagrangian method, we were able to provide some pieces of numerical evidence for the decay rate (11).
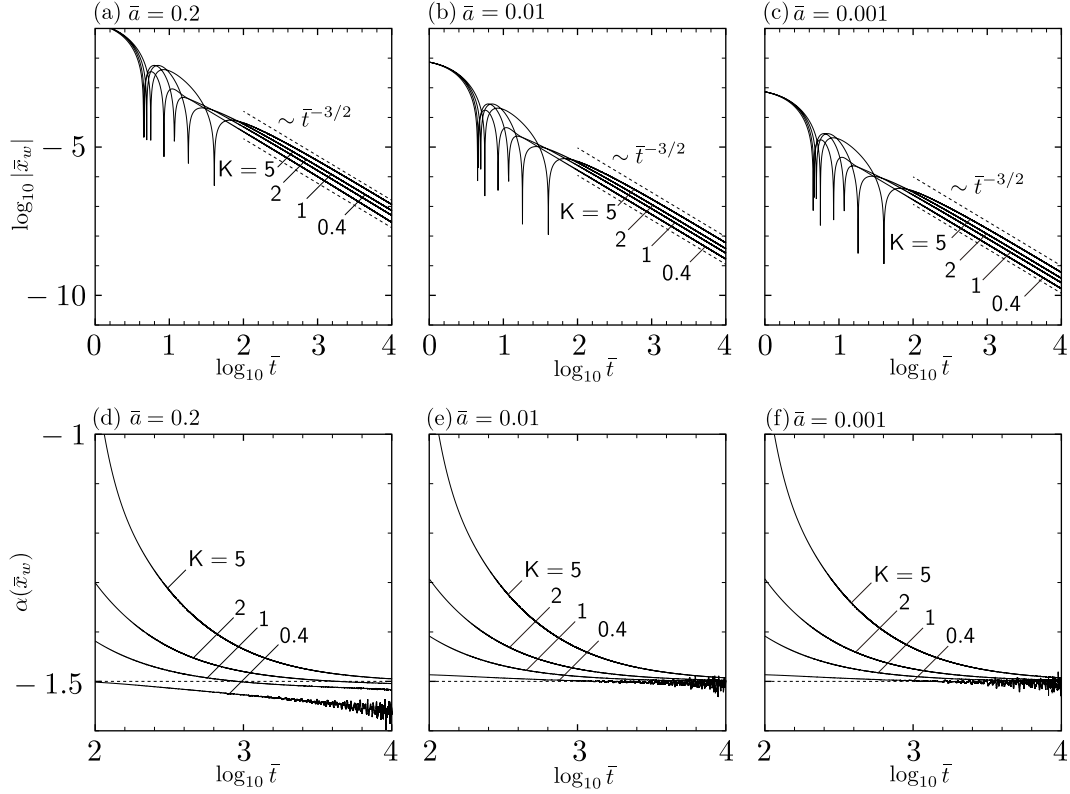
Fig. 7: $\log_{10}|\bar{x}_w|$ versus $\log_{10}\bar{t}$ for long times at several K ($\mathcal{M} = \rho_0 c_0/\omega$). (a) $\bar{a} = 0.2$, (b) $\bar{a} = 0.01$, (c) $\bar{a} = 0.001$. Panels (d), (e), and (f) show, respectively, the gradient of the curves in panels (a), (b), and (c) [cf. Eq. (12)].

Acknowledgement

[1] C. Cercignani, *The Boltzmann Equation and Its Applications* (Springer-Verlag, Berlin, 1988).

[2] Y. Sone, *Kinetic Theory and Fluid Dynamics* (Birkhäuser, Boston, 2002); see also `http://hdl.handle.net/2433/66099`.

[3] Y. Sone, *Molecular Gas Dynamics: Theory, Techniques, and Applications* (Birkhäuser, Boston, 2007); see also `http://hdl.handle.net/2433/66098`.

[4] G. A. Bird, *Molecular Gas Dynamics and the Direct Simulation of Gas Flows* (Oxford Univ. Press, Oxford, 1994).

[5] Y. Sone and S. Takata, Discontinuity of the velocity distribution function in a rarefied gas around a convex body and the S layer at the bottom of the Knudsen layer, Transp. Theory Stat. Phys. **21**, 501–530 (1992).

[6] T. Tsuji and K. Aoki, Numerical analysis of nonlinear acoustic wave propagation in a rarefied gas, in *28th International Symposium on Rarefied Gas Dynamics 2012*, AIP Conf. Proc. 1501, edited by M. Mareschal and A. Santos (AIP, Melville, 2012), pp. 115–122.

[7] T. Tsuji and K. Aoki, Moving boundary problems for a rarefied gas: Spatially one-dimensional case, J. Comp. Phys. **250**, 574–600 (2013).

[8] P.L. Bhatnagar, E.P. Gross, M. Krook, A model for collision processes in gases. I. Small amplitude processes in charged and neutral one-component systems, Phys. Rev. **94**, 511–525 (1954).

[9] P. Welander, On the temperature jump in a rarefied gas, Ark. Fys. **7**, 507–553 (1954).

[10] K. Aoki, Y. Sone, K. Nishino, and H. Sugimoto, Numerical analysis of unsteady motion of a rarefied gas caused by sudden changes of wall temperature with special interest in the propagation of a discontinuity in the velocity distribution function, in *Rarefied Gas Dynamics*, edited by A. E. Beylich (VCH, Weinheim, 1991) 222–231.

[11] T. Tsuji and K. Aoki, Gas motion in a microgap between a stationary plate and a plate oscillating in its normal direction," Microfluid. Nanofluid. **16**, 1033–1045 (2014).

[12] T. Tsuji, K. Aoki, Decay of an oscillating plate in a free-molecular gas, in *27th International Symposium on Rarefied Gas Dynamics 2010*, AIP Conf. Proc. 1333, edited by D.A. Levin, I.J. Wysong, and A.L. Garcia (AIP, Melville, 2011), pp. 140–145.

[13] T. Tsuji, K. Aoki, Decay of a linear pendulum in a free-molecular gas and in a special Lorentz gas, J. Stat. Phys. **146**, 620–645 (2012).

[14] S. Caprino, G. Cavallaro, C. Marchioro, On a microscopic model of viscous friction, Math. Models Methods Appl. Sci. **17**,1369–1403 (2007).

[15] G. Russo and F. Filbet, Semilagrangian schemes applied to moving boundary problems for the BGK model of rarefied gas dynamics, Kinet. Relat. Models **2**, 231 (2009).

[16] T. Tsuji and K. Aoki, Decay of a linear pendulum in a collisional gas: Spatially one-dimensional case, Phys. Rev. E, **89**, 052129 (2014).